Pharmaceutical Biology

ISSN: 1388-0209 (Print) 1744-5116 (Online) Journal homepage: http://www.tandfonline.com/loi/iphb20

Reduction of Candida tropicalis biofilm by photoactivation of a Heterophyllaea pustulata extract

Juliana Marioni, Julio E. Arce, José L. Cabrera, María G. Paraje & Susana C. Núñez Montoya

To cite this article: Juliana Marioni, Julio E. Arce, José L. Cabrera, María G. Paraje & Susana C. Núñez Montoya (2016): Reduction of Candida tropicalis biofilm by photoactivation of a Heterophyllaea pustulata extract, Pharmaceutical Biology, DOI: 10.1080/13880209.2016.1183683

To link to this article: http://dx.doi.org/10.1080/13880209.2016.1183683

Published online: 03 Jun 2016.

PHARMACEUTICAL BIOLOGY, 2016
http://dx.doi.org/10.1080/13880209.2016.1183683

Taylor & Francis
Taylor & Francis Group

RESEARCH ARTICLE

Reduction of *Candida tropicalis* biofilm by photoactivation of a *Heterophyllaea pustulata* extract

Juliana Marioni[a,b], Julio E. Arce[b], José L. Cabrera[a], María G. Paraje[b] and Susana C. Núñez Montoya[a]

[a]IMBIV-CONICET, Departamento De Farmacia, Facultad De Ciencias Químicas, Universidad Nacional De Córdoba, Córdoba, Argentina; [b]IMBIV-CONICET , Cátedra De Microbiología, Facultad De Ciencias Exactas Físicas Y Naturales. Universidad Nacional De Córdoba, Córdoba, Argentina

ABSTRACT

Context: Biofilm formation is an important problem, since this growth mode confers resistance to drugs usually used in therapeutics.

Objective: *In vitro* antifungal activity of extracts obtained from *Heterophyllaea pustulata* Hook f. (Rubiaceae) were studied against *Candida tropicalis* biofilms, evaluating the effect of irradiation and the oxidative and nitrosative stresses as possible mechanisms of action.

Materials and methods: Hexane, benzene, ethyl acetate and ethanol extracts were evaluated at three concentrations (0.2, 0.1 and 0.05 mg/mL) over mature biofilm, under darkness and irradiation. After 48 h of incubation, biofilm quantitation was performed by the O'Toole and Kolter method. Reactive oxygen species (ROS) was measured by nitro-blue tetrazolium (NBT) reaction and reactive nitrogen intermediates (RNI) by the Griess reagent. Superoxide dismutase activation (SOD, NBT assay) and total antioxidant system (FRAP test) were studied.

Results: Only the benzene extract at 0.2 mg/mL reduced the biofilms formation. The slight decrease achieved in darkness (17.06 ± 2.80% reduction) was increased by light action (39.31 ± 3.50% reduction), clearly observing a photostimulation. This great reduction was confirmed by confocal microscopy. In darkness, biofilm reduction was mediated by an increase in RNI, whereas under irradiation, the ROS action was most important. Although no SOD activation was observed, a strong stimulation of the total antioxidant system was detected. HPLC analysis established a high content of several anthraquinones in this extract.

Discussion and conclusion: Biofilm reduction by benzene extract was mainly mediated by oxidative stress triggered under light action, confirming a photodynamic sensitization, which could be attributed to its high content of photosensitizing anthraquinones.

ARTICLE HISTORY
Received 17 February 2016
Revised 5 April 2016
Accepted 24 April 2016
Published online 2 June 2016

KEYWORDS
Antioxidant defence system; *Candida* biofilms; HPLC analysis; nitrosative stress; oxidative stress; photosensitization; Rubiaceae

Introduction

Heterophyllaea pustulata Hook f. (Rubiaceae) is a shrub that produces photosensitization in those animals that ingest it, when the grass is scarce and causes dermatitis and blindness in the form of keratoconjunctivitis, and these symptoms are reverted back when they stop consuming it (Hansen & Martiarena, 1967). Its habitat is confined to the Andean region of Northwest Argentina and Bolivia (2000–3000 m above sea level), where it is popularly known as 'cegadera', 'ciegadera' or 'saruera', names that mean 'blindness' (Bacigalupo, 1993).

Previously, we demonstrated the *in vitro* antibacterial, antifungal and antiviral activity of some extracts of this plant, specifically against different planktonic strains, with low toxicity *in vivo* (Núñez Montoya et al. 2003; Konigheim et al. 2012). The chemical investigation of bioactive extracts revealed the predominance of 9,10-anthraquinone aglycones (AQs) (Figure 1) (Núñez Montoya et al. 2003, 2006; Konigheim et al. 2012) with demonstrated photosensitizing properties, which act by Type I (superoxide anion radical production, $O_2^{\bullet -}$) and/or Type II (singlet oxygen generation, $^1O_2$) mechanisms (Núñez Montoya et al. 2005; Comini et al. 2007).

In the last decades, opportunistic mycoses have gained health importance. These fungi have the ability to form biofilms, where both the cellular morphotypes (yeast and hyphae) are intertwined in a tridimensional exopolysaccharides matrix, which confers resistance against the antifungal agents used in current therapy (Bizerra et al. 2008). Although *Candida albicans* is the main exponent of these opportunistic fungi, in recent years *Candida tropicalis* has been isolated as one of the most prevalent pathogenic yeast species of the *Candida*-non-*albicans* group (Ramage et al. 2012; Silva et al. 2012).

One approach that is being developed for treating infections caused by fungal biofilms is antimicrobial photodynamic therapy (APDT), in which light, in the presence of oxygen, stimulates or triggers the antimicrobial effect of photosensitizing substances, by increasing their ability to generate reactive oxygen species (ROS) (Pereira Gonzaleza & Maich, 2012), which results ultimately in oxidative stress of the pathogenic microorganism. In this work, our interest was to study the *in vitro* antifungal activity of extracts with different polarity and hence, with different chemical compositions, against *C. tropicalis* biofilms, assessing specifically the light action as a trigger to increase this biological effect (photoactivation).

The ROS and reactive nitrogen intemediates (RNI) generation were studied as potential action mechanisms. Thus, $O_2^{\bullet -}$ and nitric oxide (NO) production were evaluated

CONTACT Prof. Dr. Susana C. Núñez Montoya sununez@fcq.unc.edu.ar Departamento de Farmacia, Facultad de Ciencias Químicas, IMBIV-CONICET. Universidad Nacional de Córdoba, Haya de la Torre y Medina Allende, X5000HUA Córdoba, Argentina

Supplemental data for this article can be accessed here.

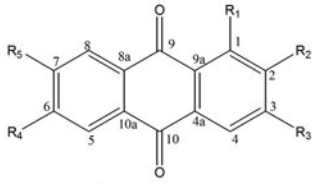

Anthraquinone nucleus

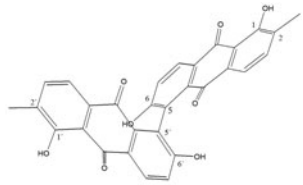

5,5'-Bisoranjidiol (9)

Anthraquinones	R_1	R_2	R_3	R_4	R_5
Rubiadin (**1**)	OH	Me	OH	H	H
Soranjidiol (**2**)	OH	Me	H	OH	H
Rubiadin-1-methyl ether (**3**)	OMe	Me	OH	H	H
Soranjidiol-1-methyl ether (**4**)	OMe	Me	H	OH	H
2-Hydroxy-3-methyl anthraquinone (**5**)	H	OH	Me	H	H
Damnacanthol (**6**)	OMe	CH_2-OH	OH	H	H
Heterophylline (**7**)	OH	Me	H	OH	OMe
Pustuline (**8**)	H	OH	OMe	H	Me

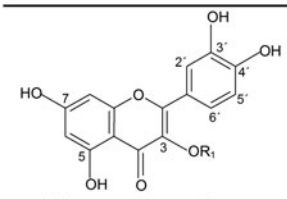

Flavonoids nucleus

Flavonoid	R_1
Quercetin (**10**)	H
Isoquercitrin (**11**)	D-glucose
Quercetin-3-*O*-*β*-D-(6"-acetylglucosyl) (**12**)	6-*O*-acetyl-D-glucose

Figure 1. Structure of identified compounds in *Heterophyllaea pustulata* extracts.

simultaneously, as the main precursor of ROS and RNI, respectively (Powers et al. 2011). In both kinds of stresses, there is an overproduction of reactive species, which can be caused by a stimulation in their production or a reduction in antioxidant defence system. Consequently, the total antioxidant capacity of the system was evaluated (enzymatic and non-enzymatic) as a response to both kinds of stresses, by means of the FRAP assay (ferrous reduction antioxidant potency). In addition, the activation of the superoxide dismutase enzyme (SOD) was studied because of its specific action over $O_2^{\bullet -}$, it catalyzes the dismutation of superoxide into hydrogen peroxide (H_2O_2).

Materials and methods

Yeast strain, chemicals and biochemicals

Clinical isolates of *C. tropicalis* were kindly provided and identified by the Microbiology Laboratory of Clínica Universitaria Reina Fabiola (Córdoba, Argentina). Stock cultures were preserved at −80 °C using 20% glycerol (v/v) as cryoprotectant. Standards AQs and flavonoids were purified by our research group, and identified by means of its spectral data (UV-V, IR, MS, one- and two-dimensional NMR) (Núñez Montoya, 2002; Núñez Montoya et al. 2003, 2006). We used the following reagents: Crystal violet (CV, Anedra, Tigre, Argentina); Fetal Bovine Serum (FBS, Greiner Bio-One, Frickenhausen, Germany); Sabouraud Dextrose Broth (SDB, Britania, Buenos Aires, Argentina); Phosphate Buffer Solution (PBS); dimethyl sulfoxide (DMSO, Merck, Darmstadt, Germany); amphotericin B (Amp-B, Sigma-Aldrich, ≥80%, St Louis, MO); Calcofluor-White (Sigma-Aldrich Co, St Louis, MO); Nitro Blue Tetrazolium (NBT, Sigma-Aldrich); sulfanilamide (Anedra); HCl (Anedra); N-1-naphthyl ethylenediamide dihidrochloride (Sigma-Aldrich); $NaNO_2$ (Sigma-Aldrich); methionine (Sigma-Aldrich); riboflavin (Sigma-Aldrich); 2,4,6-tripyridyl-s-triazine (Sigma-Aldrich); $FeCl_3 \cdot 6H_2O$ (Cicarelli, Santa Fé, Argentina); $FeSO_4$ (Cicarelli); formic acid (Anedra); NaOH (Anedra). The solvents were distilled before use. Distilled or ultrapure water was used whenever necessary.

Plant material and preparation of extracts

Vegetal material was collected in El Alisal (Department of Rosario de Lerma, Salta province, Argentina) in February 2013. A voucher specimen was deposited at Museo Botánico de Córdoba

(Universidad Nacional de Córdoba) as J. Micheloud s/n, CORD 19759. Dried aerial parts (270 g) were crushed and then successively extracted in a Soxhlet apparatus using solvents of increasing polarity (Núñez Montoya, 2002; Núñez Montoya et al. 2003) to obtain the following dried extracts: hexane (Hex, 1.2976 g) benzene (Ben, 0.7907 g), ethyl acetate (EtOAc, 1.0051 g) and ethanol (EtOH, 8.0638 g). Thus, a wide range of secondary metabolites separated by their polarity were obtained.

Biofilm formation assay

The biofilms-forming ability of the clinic strains were measured using an assay adapted from the method of O'Toole and Kolter (1998), which is based on the facility of strains to form biofilms on solid surfaces and uses CV to stain. The assay was adjusted to 96-well microtiter plates (Greiner Bio-One, Germany) according to previously published procedure (Arce Miranda et al. 2011; Peralta et al. 2015). Briefly, plates were pretreated with 50% FBS in SDB at 37 °C for 30 min and washed with 10 mM PBS (pH 7.2) twice. Then, a cell suspension in SDB (1×10^7 cells/mL, pH = 6.5 adjusted with 0.1 M NaOH) was inoculated and plates were incubated at 37 °C for 48 h without shaking to allow the attachment of cells on the surface. Control wells were pre-treated with FBS and contained only SDB (pH = 6.5). After incubation, non-adhered cells were removed by washing the wells with sterile PBS. Then, plates were air dried for 24 h prior to CV (1% w/v) staining. Adherent biofilms were washed with water to remove unbound dye. Finally, CV was extracted with the bleaching solution (0.2 mL): ethanol–glacial acetone (70:30). The optical density (OD) was determined at 595 nm using a microplate reader (Tecan Sunrise Model, TECAN, Australia). The average OD of the strain was compared with average OD of the control wells (ODc), both reported as means ± standard deviations. Strains were classified according to its ability to form biofilm by following these criteria: $OD \leq ODc$ = no biofilm producer; $ODc < OD \leq (2 \times ODc)$ = weak biofilm producer, $(2 \times ODc) < OD \leq (4 \times ODc)$ = moderate biofilm producer and $(4 \times ODc) < OD$ = strong biofilm producer. Isolates classified as strong biofilm producer, were selected to be used in the *in vitro* antifungal activity test. The amount of formed biofilm was expressed as biofilm biomass unit (BBU), which was arbitrarily defined as 0.1 OD_{595} equal to 1 BBU (Arce Miranda et al. 2011; Peralta et al. 2015).

In vitro *antifungal activity assay over biofilms*

From a stock solution of each dried extract (1 mg/mL) in SDB (pH = 6.5) that contained 1% DMSO as co-solvent, three dilutions were prepared (0.2, 0.1 and 0.05 mg/mL). Antifungal activity was determined over the biofilms formed as described earlier, using specifically the single strain classified as a strong biofilm producer with a BBU level of 32.22 ± 2.86 ($p < 0.05$). Following growth, biofilms were washed with sterile PBS and the three concentrations of each extract were added in triplicate. Wells containing only SDB (DMSO 1%, pH = 6.5) were considered as controls. Amp-B was used as the positive control at 0.5 µg/mL, which is its minimal inhibitory concentration (MIC) determined for planktonic cells, according to the protocols of the Clinical and Laboratory Standards Institute (CLSI, 2008). Two microplates were simultaneously performed under darkness and irradiated for 15 min. After that, both microplates were incubated at 37 °C for 48 h. Then, the supernatant was removed in order to measure the production of ROS and RNI, the SOD activity, and the total antioxidant activity of the biological system by FRAP assay. After removing the supernatant, the biofilm formation was quantified and the results were expressed as BBU (0.1 $OD_{595\,nm} = 1$ BBU) (O'Toole & Kolter, 1998; Arce Miranda et al. 2011; Peralta et al. 2015). The percentage of reduction was calculated using the following formula:

$$\%\,R = \frac{\text{Control } OD_{595nm} - \text{Text } OD_{595nm}}{\text{Control } OD_{595nm}} \times 100$$

Irradiation system comprised a 20W Phillips actinic lamp (380–480 nm, 0.65 mW/cm^2) with an emission maximum at 420 nm, placed inside a black box at 20 cm above the samples. The maximum concentrations that inhibited the formation of biofilm were defined as the biofilm inhibitory concentration (BIC) (Nithyanand et al. 2015).

Confocal laser scanning microscopy (CLSM)

C. tropicalis biofilms were formed on small glass covers (12 mm diameter) in a 24-well microtiter plate (Greiner Bio-One, Frickenhausen, Germany). Matured biofilms were incubated with Ben extract at its BIC (0.2 mg/mL) under darkness and irradiation (15 min). Then, disks were stained with 30 µL of Calcofluor-White (0.05% v/v, Sigma-Aldrich) for 1 min. Calcofluor-White, a carbohydrate-binding fluorescent dye that stains the cell walls of fungi blue , was excited at 355 nm (Peralta et al. 2015). Disks were air-dried for 15 min in darkness and were placed inverted in 35 mm glass-bottom microwell dishes. Intact biofilms were examined using a Fluoview FV1000 Espectral Olympus CSLM (Olympus Latin America, Miami, FL), equipped with UPlanSApo 100X/1.40 oil UIS2 Olympus oil immersion lens. Optical sections were acquired at 0.5 µm intervals for the total thickness of biofilms. The reduction in total biomass and maximum thickness of *C. tropicalis* biofilm was assessed using COMSTAT software (Technical University of Denmark: Kongens Lyngby, Denmark).

Reactive oxygen species production

ROS were detected by their oxidative action that causes the nitro blue tetrazolium (NBT) reduction to nitroblue diformazan, by following the methodology previously described by us (Paraje et al. 2009; Arce Miranda et al. 2011; Peralta et al. 2015). Since the by-product of this assay is proportional to the ROS generated in biofilms, its absorbance was measured at 540 nm in the same microplate reader used earlier. Results were expressed as Abs_{540nm}/BBU (ROS/BBU).

Reactive nitrogen intermediates generation

NO generation (precursor of RNI) was evaluated as nitrite by a microplate assay using the Griess reagent (Paraje et al. 2009; Arce Miranda et al. 2011). The OD at 540 nm of each well was measured with an automated microplate reader used before. The concentration of nitrite was calculated from an $NaNO_2$ standard curve and expressed in micromolars (µM) (Arce Miranda et al. 2011). Results were expressed as the nitrite concentration value/BBU (RNI/BBU).

Superoxide dismutase activity

Total SOD activity was photochemically assayed, based on the ability of SOD to inhibit the reduction of NBT by the $O_2^{\bullet -}$ generated through the illumination of riboflavin in the presence of

oxygen and the electron donor methionine. Results were expressed as SOD activation percentage compared to control (100%)/BBU (SOD activation/BBU) (Baronetti et al. 2013).

Antioxidant capacity assays

This assay measures the reducing potential of a biological system by means of its reaction with a complex of ferric tripyridyltriazine [Fe^{3+}-TPTZ] that produces a coloured compound: ferrous tripyridyltriazine [Fe^{2+}-TPTZ]. Absorbance was measured at 593 nm using the same microplate reader mentioned earlier. The FRAP values were calculated using an $FeSO_4$ calibration curve and expressed in μM (Benzie & Strain, 1996). Results were expressed as the Fe^{+2} concentration values/BBU (FRAP/BBU).

Statistical analyses

All biological experiments were performed in triplicate and in three independent experiments, and the averages and standard deviations were calculated for all experiments. Results were plotted as means values with error bars that represent standard deviations. Data were statistically analyzed using ANOVA followed by the Student–Newman–Keuls test for multiple comparisons. The differences were considered to be statistically significant at p value <0.05.

HPLC analysis

A Varian Pro Star chromatography apparatus (model 210, series 04171, California, USA), equipped with a UV-Vis detector was used. The separation was achieved on a Microsorb-MV column 100-5 C-18 (250 × 4.6 mm i.d., Agilent), at 25 °C. The mobile phase involved formic acid (0.16 M, solvent A) and MeOH-formic acid (0.16 M, solvent B), starting with 48% B (2 min, 1.0 mL/min) that changed during 4 min to 78% and 0.8 mL/min (2 min), followed by a second ramp (2 min) to 84% B and 0.5 mL/min (30 min), a third ramp (1 min) to 100% B and 0.7 mL/min (4 min), returning to the starting conditions for 1 min. Detector was set at 269 nm. The manual injection volume was 20 μL. Data analysis was performed using Varian software (Star Chromatography Workstation 6.41, California, USA). Each dried extract and each reference compound was accurately weighed, and then it was dissolved in necessary volume of MeOH (HPLC, Sintorgan) to obtain the corresponding solutions of 1 mg/mL (sample and standards), which were filtered through paper filter Whatman No. 1 (micro filtration system).

Identification was carried out by comparing the HPLC retention times (t_R) with the corresponding standard compound and co-chromatography with added standards. The t_R values of each identified metabolite were expressed as means ± SD from three injections for each sample.

Quantitation was achieved by external calibration method. The concentration of each identified AQ was expressed as rubiadin (**1**), and the amount of every detected flavonoid as quercetin (**10**) (Figure 1). A calibration curve was made for each reference standard separately (**1** and **10**, 94–96% purity), by plotting the area under each peak (AUP) as a function of each analyte concentration. From a stock solution of each analyte (1 mg/mL) in MeOH (HPLC), five consecutive dilutions (1:2) were prepared in the range of $0.10–6.25 \times 10^{-3}$ mg/mL for standard **1**, and $0.20–1.25 \times 10^{-2}$ mg/mL for standard **10**. The stock solution was prepared in triplicate in order to obtain three replicates of each dilution, so that each five-pointed curve was constructed in triplicate on two consecutive days, and all stock and working solutions were kept at −20 °C. A linear regression analysis was performed, in which the minimum acceptable value for the correlation coefficient (R^2) of the curve was 0.99 or more. Using the calibration curve of rubiadin (**1**), the concentration of each AQ in the extracts was estimated by interpolating the AUP for each compound; and the same procedure was performed to establish the amount of flavonoids in extracts, but using the calibration curve of quercetin (**10**). Then, the concentration of each identified compound was expressed in % w/w based on dried extract.

HPLC validation

A series of assays were performed to ensure that the validation method complies with the FDA Guidelines (International Conference on Harmonization, 2005a, b), such as the determination of selectivity, linearity and linear range, limits of detection (LOD) and quantitation (LOQ), and intra-day and inter-day precision and accuracy. The selectivity was given by the chosen wavelength (λ) for detecting only the compounds of interest, without the interference of other compounds. The linearity of working curve was checked by verifying compliance with the Lambert–Beer law in the range of tested concentrations for each standard compounds (**1** and **10**), and it was expressed as $R^2 \geq 0.99$. The LOD and LOQ values of each reference compounds (**1** and **10**) were determined from the y-intercept standard deviation (Sb) and the slope (a) of a calibration curve achieved by diluting standard solutions sequentially of the corresponding compounds (Quattrocchi et al. 1992).

The intra- and inter-day precision and accuracy of the chromatographic system were evaluated using two concentrations of each analyte (**1** and **10**) selected from the respective calibration curves (within the linearity range), and each concentration were prepared in triplicate by diluting different stock solutions prepared as described earlier. The two known concentration solutions of each reference standard, each one in triplicate, were analyzed in the same day (repeatability) and in three consecutive days (reproducibility). The acceptability criteria for intra- and inter-day precision was the relative standard deviation (% RSD) for each tested concentration, which should not exceed the maximum value of RSD calculated by the Horwitz equation ($RSDmax = 2^{(1-0.5\log C)}$, where C is the LOD of each analyte expressed in base 10 logarithm (Horwitz, 1982).

The intra- and inter-day precisions of the analytical procedure, together with accuracy (recovery) for the two analytes were assessed by spiking the Ben extract with standard **1** (45 μg/mL) and the EtOAc extract with reference **10** (30 μg/mL). Those were performed by following the method applied to the sample analysis for three consecutive days. The variations were evaluated using the RSD of triplicate injections. The accuracy of the method was evaluated by analyzing the recovery percentage of compounds **1** in Ben extract and compound **10** in EtOAc extract. The recovery percentage was calculated using the ratio of contents detected (actual) to those added (theoretical).

Results and Discussion

In vitro *antifungal activity on* Candida tropicalis *biofilms*

Under darkness, the Ben extract induced a slight decrease in the BBU only at the highest tested concentration (0.2 mg/mL), and this effect was increased by the light action (Figure 2). Thus, the

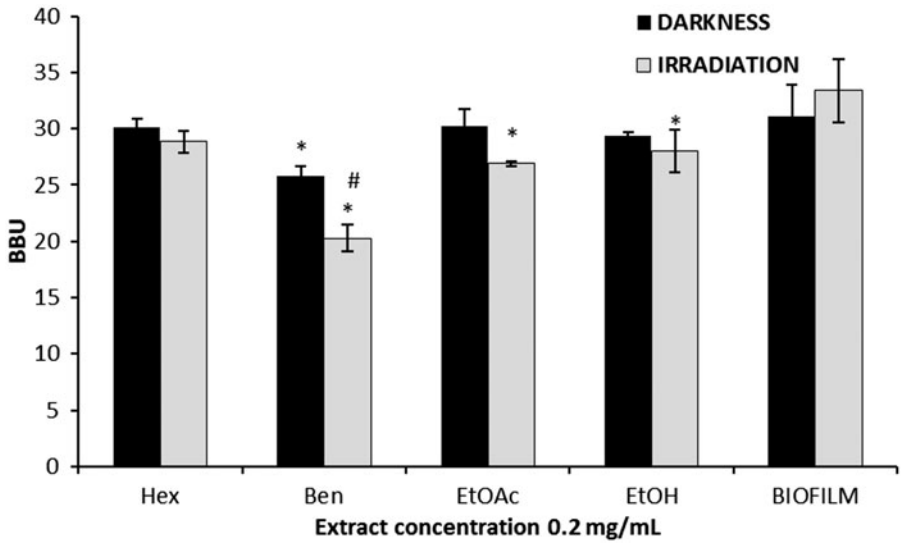

Figure 2. *In vitro* antifungal activity of extracts obtained from *H. pustulata* against *C. tropicalis* biofilms, expressed as BBU, under darkness and irradiation conditions. Error bars represent the standard deviations of the means of three independent experiments with $n = 3$. *Denotes statistical significance at $p < 0.05$ when compared to untreated biofilms. #indicates statistical significance at $p < 0.05$ when darkness and irradiation were compared. Hex: Hexane extract; Ben: Benzene extract; EtOAc: Ethyl acetate extract; EtOH: Ethanol extract.

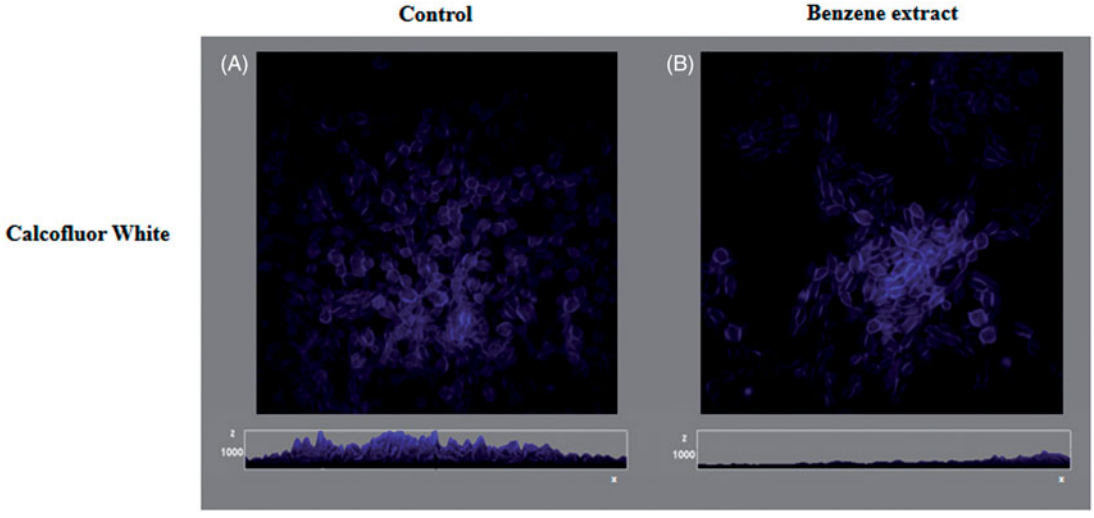

Figure 3. CSLM images showing the antifungal activity of benzene extract against *C. tropicalis* biofilms. Blue channel shows Calcofluor in sessile cells walls. (A) Postive control, (B) Benzene extract (0.2 mg/mL). Magnification 60× and scale bar is 10 μm.

obtained BBU in presence of the Ben extract and light (20.26 ± 1.18) were almost two times lower than biofilm control (33.38 ± 2.80), which represents a reduction percentage (%*R*) of 39.31 ± 3.50 versus 17.06 ± 2.80%*R* in darkness ($p < 0.05$). It should be noted that during the experiment, the light did not have any inhibitory effect on the biofilms growth, and DMSO control did not show any antifungal activity (data not shown). The other extracts were not active in the dark at any tested concentration, since no decrease was observed in the BBU in comparison with the biofilm control (data not shown). Under irradiation, the AcOEt and EtOH extracts also reduced the BBU only at the highest assayed concentration, but this decrease was not significant as compared with the same condition in darkness (data not shown).

Therefore, only the Ben extract was able to reduce the biofilm formation of *C. tropicalis* by means of a photo-stimulated effect, establishing that the maximum concentrations inhibiting the biofilm was 0.2 mg/mL in both the experimental conditions (dark and irradiation), which was defined as the BIC (Nithyanand et al. 2015).

Confocal laser scanning microscopy (CLSM)

CLSM confirmed the activity of Ben extract on *C. tropicalis* biofilm under darkness and irradiation. Figures 3(A,B) show laser scanning fluorescence images for XY (top) and XZ (bottom) of sessile cells of *Candida* biofilm (blue). CLSM images showed the reduction in the thickness of the biofilms treated with Ben extract at BIC under irradiation (Figure 3(B)), when compared to the control (Figure 3(A)). COMSTAT analysis showed that the biofilm biomass and the thickness were reduced upon treatment with Ben extract (biofilm thickness 12.96 μm, 38% of reduction) when compared to the control (biofilm thickness 20.86 μm). This result showed correlation with the CV assay.

The results obtained by CV and CLSM demonstrated that only the Ben extract at 0.2 mg/mL (BIC) was able to reduce the biofilm formation of *C. tropicalis*, and this reduction was more important under light action, noting a photo-stimulation of the antifungal effect. In order to establish the possible mechanism by which the

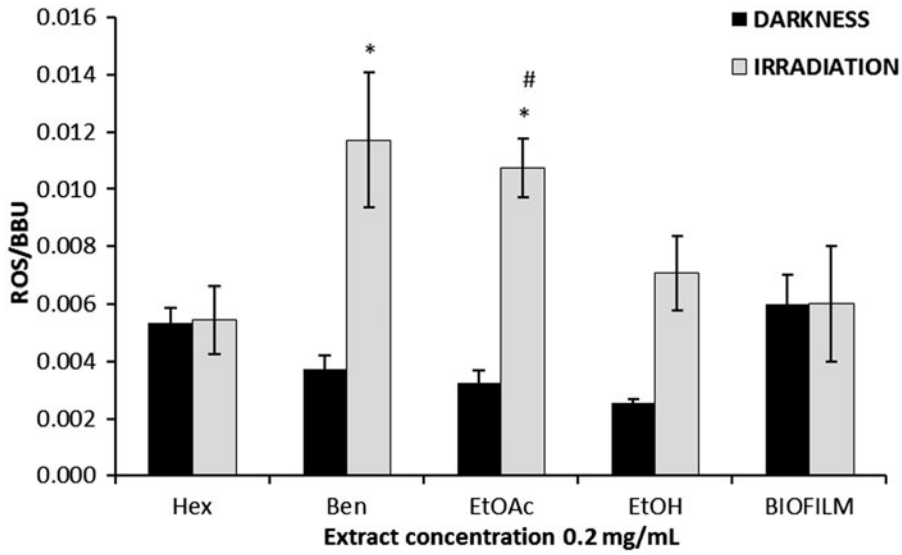

Figure 4. Reactive oxygen species (ROS) generation by *H. pustulata* extracts in *C. tropicalis* biofilms, under darkness and irradiation. ROS and BBU ratio (ROS/BBU) determined by NBT assay. Error bars represent the standard deviations of the means of three independent experiments with $n = 3$. *Denotes statistical significance at $p < 0.05$ when compared to untreated biofilms. #indicates statistical significance at $p < 0.05$ when darkness and irradiation were compared. Hex: Hexane extract; Ben: Benzene extract; EtOAc: Ethyl acetate extract; EtOH: Ethanol extract.

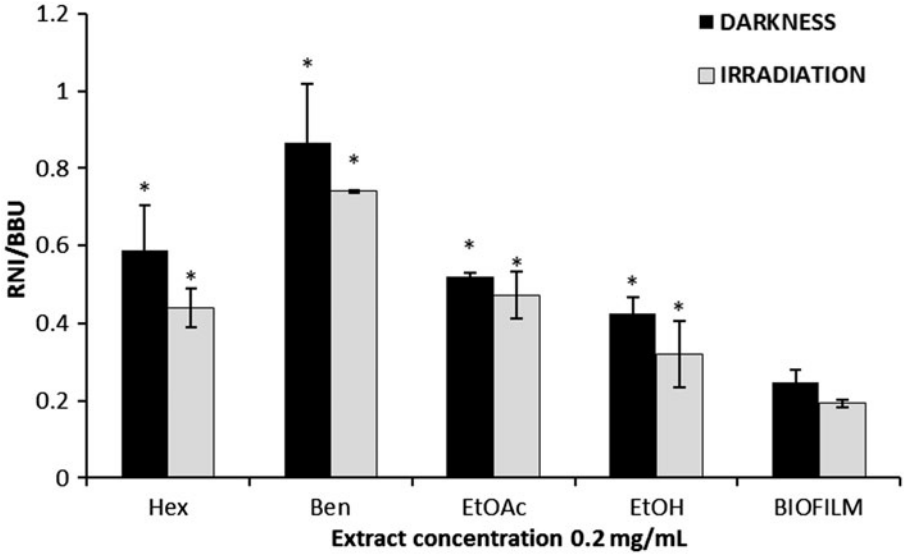

Figure 5. Nitric oxide (NO) production induced by *H. pustulata* extracts in *C. tropicalis* biofilms, under darkness and irradiation. RNI and BBU ratio (RNI/BBU) determined by Griess test. Error bars represent the standard deviations of the means of three independent experiments with $n = 3$. *Denotes statistical significance at $p < 0.05$ when compared to untreated biofilms. #indicates statistical significance at $p < 0.05$ when darkness and irradiation were compared. Hex: Hexane extract; Ben: Benzene extract; EtOAc: Ethyl acetate extract; EtOH: Ethanol extract.

observed effect is produced, the ROS and RNI generation were studied under both the experimental conditions (darkness and irradiation).

ROS generation

ROS production in the dark was not increased by any tested extracts (Figure 4), so another action mechanism would be involved in the reducing effect of the Ben extract against the biofilms under this experimental condition. When the biological system was irradiated, the Ben extract showed the largest increase in ROS, which was almost 2-fold higher than the biofilm control (0.0117 ± 0.0023 versus 0.0060 ± 0.0020) and generated an increase in more than 3-fold of its production in darkness (0.0037 ± 0.0005).

RNI production

In both the conditions of work, the Ben extract stood out for producing the highest stimulation of RNI (Figure 5). Since in darkness no ROS production was noted (Figure 4), but there was an increase in the RNI generation (3.5 times RNI/BBU with respect to biofilm), we infer that these reactive species would be responsible for the slight effect that Ben extract has on the biofilm under this experimental condition ($17.06 \pm 2.80\%$R) (Figure 2). The RNI production under irradiation was similar or lower than the level generated in the dark by all extracts, and this increase showed no effect against biofilms in darkness (except that generated by the Ben extract). Considering these results, we might infer that the RNI generation is not the primary mechanism involved in biofilms reduction, but the increase in ROS would be the main cause of decreased biofilms under irradiation (Figures 2 and 4).

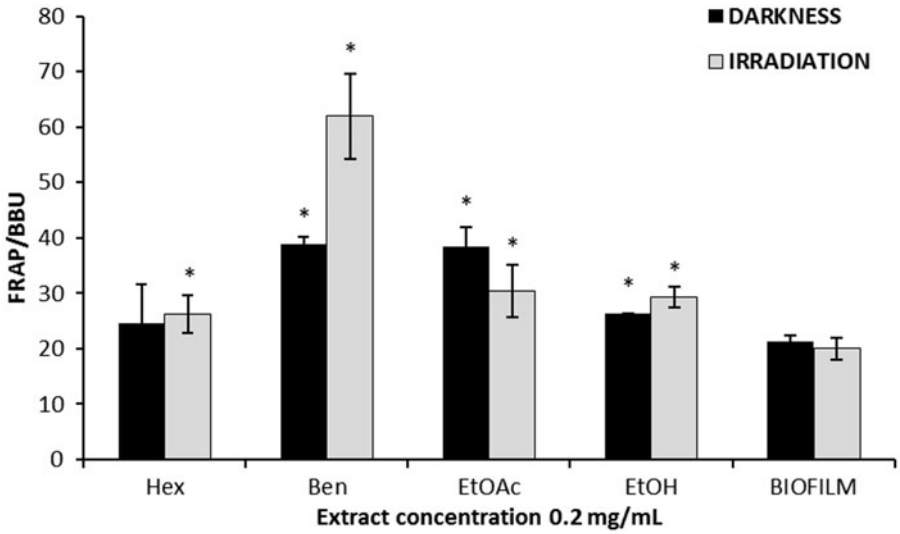

Figure 6. Activation of the total antioxidant system in *C. tropicalis* biofilms by *H. pustulata* extracts, under darkness and irradiation. FRAP and BBU ratio (FRAP/BBU). Error bars represent the standard deviations of the means of three independent experiments with $n = 3$. *Denotes statistical significance at $p < 0.05$ when compared to untreated biofilms. #indicates statistical significance at $p < 0.05$ when darkness and irradiation were compared. Hex: Hexane extract; Ben: Benzene extract; EtOAc: Ethyl acetate extract; EtOH: Ethanol extract.

Although we could not establish a direct relationship between the generated RNI and the biofilms reduction by the action of light, we do not rule out that they may contribute indirectly, especially in the case of the Ben extract. It is well-known that an overproduction of $O_2^{\bullet -}$ promotes its reaction with NO to generate peroxynitrite ($ONOO^-$), a highly reactive species (Powers et al. 2011). Thus, the NO acts as a $O_2^{\bullet -}$ quencher, by playing a prooxidant role that is directly dependent on the $O_2^{\bullet -}$ concentration, by means of a fast non-enzymatic reaction that increases the nitrosative and oxidative processes, which generate and promote cell damages. Therefore, there would be a competition between NO and SOD by the $O_2^{\bullet -}$. Consequently, the SOD activity was evaluated under both the experimental conditions.

Superoxide dismutase activation

In the two experimental conditions, SOD activity was not increased by any extract (data not shown). Since SOD values in the treated biofilms were similar to the control (only biofilms), it means that all the $O_2^{\bullet -}$ generated by the riboflavin added in this test reacts with the enzyme, and there is no other source of ROS production. This is true for darkness situation because none of the assayed extracts stimulated the $O_2^{\bullet -}$ generation (Figure 4). However, with light some extracts increased the $O_2^{\bullet -}$ production, and also no stimulation of SOD was observed. Therefore, it can be inferred that another deactivation pathway of the $O_2^{\bullet -}$ is acting, and in this case it would be its reaction with the NO to generate $ONOO^-$, especially if we consider the reaction between radical–radical ($O_2^{\bullet -}$ and NO) is faster than the reaction between the $O_2^{\bullet -}$ and SOD (Powers et al. 2011).

Therefore, we have shown that when the biofilm was irradiated in the presence of Ben extract, a significant increase in ROS was mainly occured, which was also joined by an increase in the RNI. This would be because the NO, faced with an overproduction of $O_2^{\bullet -}$, tends to react quickly with it in its role of ROS quencher, generating $ONOO^-$. Since there was no increase in the SOD activity under this experimental condition, we can deduce that the $O_2^{\bullet -}$ deactivation by means of the radical – radical reaction ($O_2^{\bullet -}$ and NO) and was favoured over the reaction between $O_2^{\bullet -}$ and SOD, which is slower than the non-enzymatic reaction (Powers et al. 2011).

Total antioxidant capacity activation

Faced with an overproduction of reactive species (ROS and RNI), it is necessary to assess the total antioxidant response of the biological system (enzymatic and non-enzymatic) (Missall et al. 2004), which tends to counteract the generation of ROS and RNI in order to minimize the cell damage. The total antioxidant system was activated with different values (FRAP/BBU) by the action of each extract tested under both the working conditions (darkness and irradiation). The extracts of Hex, EtOAc and EtOH produced low values of activation in both the experimental conditions (Figure 6), whereas the Ben extract induced a great stimulation of the total antioxidant system. In darkness, the detected activation of the total antioxidant system seems to be enough to offset the RNI generated by the Hex, EtOAc and EtOH extracts (Figure 5), since no reducing effect against biofilms was observed (Figure 2). On the other hand, this activation was not sufficient for Ben extract that triggered a reduction in the biofilm mediated by RNI as has already been proposed. The slight stimulation of total antioxidant system produced by Hex, EtOAc and EtOH extracts under irradiation seems to counteract the effect of the ROS and RNI completely for the Hex extract that resulted inactive, or partially in the case of the EtOAc and EtOH extracts that produced a small reduction in the biofilm growth, but it was not enough to observe a photo-activated effect. By contrast, the total antioxidant system activation in the presence of light and Ben extract was not able to stabilize the reactive species generated, causing a significant reduction in the biofilms formation and observing a photo-stimulated action. Obviously, the total antioxidant system acts as a defence, and thus the biofilm eradication was not achieved.

Validation of HPLC analysis

In order to establish the chemical nature of the compounds present in the bioactive extract, an HPLC method was developed to

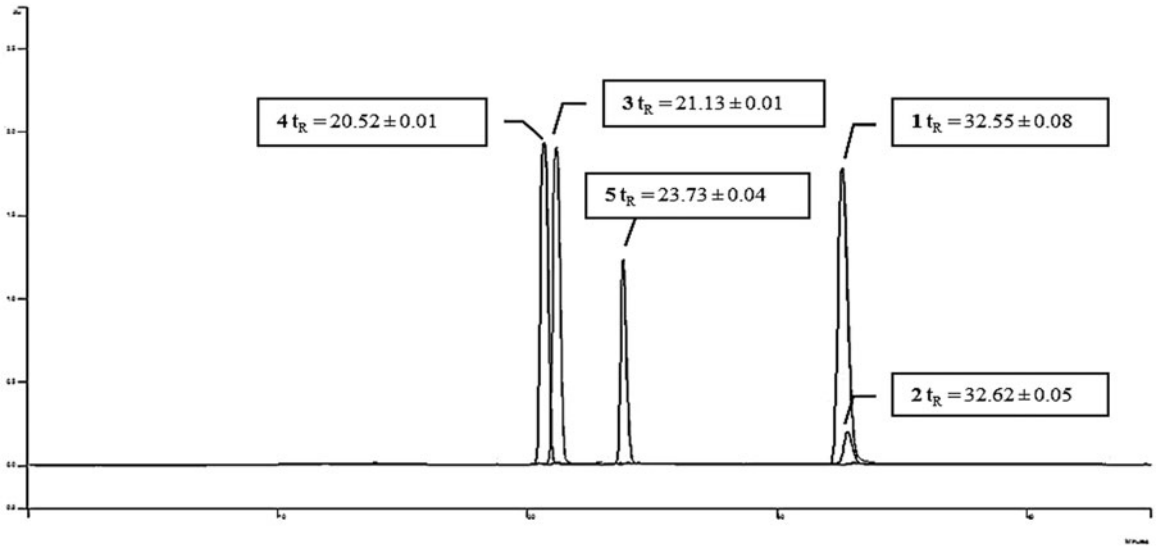

Figure 7. Overlay of chromatographic profiles of standard compound solutions. **1** (Rubiadin), **3** (Rubiadin 1-methyl ether), **4** (Soranjidiol 1-methyl ether) and **5** (2-hydroxy-3-methyl antraquinone) at 1 mg/mL, and **2** (Soranjidiol) at 125 μg/mL.

Table 1. Calibration curves, limits of detection (LOD) and quantification (LOQ) data of rubiadin (**1**) and quercetin (**10**) determined by HPLC.

Standard compounds	Linearity range (μg/mL)	Calibration equation[a]	R^2	LOD (μg/mL)	LOQ (μg/mL)
1	6.25–100	$y = 59334x + 71$	0.9953*	0.22	0.43
10	12.5–200	$y = 57994x - 527.04$	0.997*	1.12	1.63

[a]Five data points ($n = 2$), x = concentration of compounds (mg/mL) y = peak area.
*t-test: $p < 0.05$.

study the chemical composition of the extracts tested on *C. tropicalis* biofilms, specifically regarding the content of AQs and flavonoids. Previous studies showed that derivatives of these families of chemical compounds characterize this plant species, being the AQs aglycons, the majority secondary metabolites (Núñez Montoya et al. 2003, 2006).

The HPLC column and the solvent system used in the experiment were routinely applied to the separation of AQs in a complicated plant matrix (Dongxiu et al. 2009; Panichayupakaranant et al. 2009; Wei et al. 2013). In our experiment, the gradient solvent system and flow rate were optimized in order to obtain a good separation and resolution of target compounds in the chromatograms. Formic acid (0.16 M) was added to the mobile phase to reduce the peak tailing, and thus produce a symmetrical peak shape. This can be observed in the chromatographic profiles of five reference compounds, which are overlaid in Figure 7. Despite all experimental conditions tested, the separation of **1** and **2** was not achieved, which are positional isomers (Figures 7 and 1). However, its methylated derivatives in the 1-position showed good resolution (**3** and **4**). The solution of **1** was diluted in order to observe that this compound elutes at the same t_R of **2**.

The 269 nm was selected for detection of anthraquinone and flavonoid derivatives, since AQs show a maximum absorption of approximately 270 nm and the target flavonoids exhibited a maximum absorption at 258 nm with a shoulder at 269 nm (Núñez Montoya, 2002). No interference was observed for compounds in the chromatograms of the samples.

Since the concentration of each identified AQ was expressed in terms of rubiadin (**1**) and each flavonoid as quercetin (**10**), two calibration curves were performed, one for each standard compound. The equation obtained for each calibration curves and their linear correlation coefficient (R^2) are shown in Table 1, these data demonstrated the fulfillment with the Lambert–Beer law in the range of concentrations tested, and together with the t-test results confirmed that the method is linear.

To ensure the precision and accuracy of the analytical method developed in this work, a comprehensive validation study was conducted, including the chromatographic system used. Therefore, a series of assays were performed, including the determination of LOD, LOQ, linearity, intra-day and inter-day precision, and accuracy. The measurement of LOD and LOQ values of standards **1** and **10** was conducted by diluting standard solutions of the corresponding compounds sequentially. The LOD (signal-to-noise ratio = 3) and LOQ (S/N = 10) values for each reference compound are also shown in Table 1.

Intra- and inter-day variations of the two reference compounds (**1** and **10**), were used to determine precision and accuracy of the chromatographic system (Table 2). Intra- and inter-day RSD for the analytes were less than 4%, values that were less than the maximum RSD calculated by the Horwitz equation ($RSD_{max} = 16.85$ for **1** and 14.93 for **10**). These results demonstrated a good repeatability and reproducibility for this system. Moreover, a good accuracy was observed (%RSD <3). As these experiments were needed to be conducted on three consecutive days, the stability of standard **1** and **10** in working solutions was also studied at the same time. The data showed that rubiadin and quercetin in solution were stable within 3 days after preparation, kept for 8 h at room temperature and 12 h at −20 °C (Table 2).

Intra- and inter-day precisions of the proposed HPLC analytical method, expressed as percentage RSD, were investigated by triplicate injections of samples on three consecutive days. The results showed that the RSD values of intra- and inter-day precisions were less than 4% (Table 3). Therefore, the analytical method showed a good repeatability and reproducibility.

The accuracy, expressed as a recovery percentage, was determined by spiking the Ben extract with **1** and the EtOAc extract with **10**. The obtained percentage recoveries of both the analytes are shown in Table 4, which established that the method showed a good accuracy. This validation study demonstrated that the proposed HPLC method is reasonably precise and accurate for

Table 2. Intra- and inter-day precision and accuracy values for reference compounds.

Reference standards	Concentration (μg/mL)	Intra-day precision ($n = 3$) (Repeatability) Day 1 μg/mL	RSD %	Day 2 μg/mL	RSD %	Day 3 μg/mL	RSD %	Inter-day precision ($n = 9$) (Reproducibility) μg/mL	RSD %	Intra-day accuracy Day 1 RSD %	Day 2 RSD%	Day 3 RSD%	Inter-day accuracy RSD %
Rubiadin (**1**)	50	51.2 ± 1.9	3.71	51.9 ± 2.0	2.91	51.4 ± 0.7	1.36	51.5 ± 0.3	0.58	2.33	3.62	2.78	2.91
	6.25	6.43 ± 0.16	2.49	6.27 ± 0.17	1.87	6.40 ± 0.10	1.56	6.37 ± 0.07	1.09	2.75	0.40	2.41	1.87
Quercetin (**10**)	100	98.4 ± 0.9	0.91	99.6 ± 0.6	−1.33	98.1 ± 0.7	0.71	98.7 ± 0.6	0.64	−1.59	−0.44	−1.95	−1.33
	50	49.1 ± 0.7	1.43	49.3 ± 0.8	−1.74	49.0 ± 0.9	1.84	49.13 ± 0.09	0.24	−1.76	−1.49	−1.96	−1.74
		t_R (min)	RSD %	t_R (min)	RSD %	t_R (min)	RSD %	t_R (min)	RSD %				
Rubiadin (**1**)	50 and 6.25	33.16 ± 0.12	0.36	33.01 ± 0.05	0.15	32.52 ± 0.15	0.46	32.89 ± 0.34	1.03				
Quercetin (**10**)	100 and 50	12.78 ± 0.02	0.15	12.73 ± 0.06	0.47	13.03 ± 0.13	0.99	12.85 ± 0.13	1.01				

Table 3. Intra- and inter-day precision data for detected rubiadin and quercetin in the extracts of *H. pustulata*.

Compound	Intra-day precision ($n = 3$) Day 1 Content (μg/mL)	RSD (%)	Day 2 Content (μg/mL)	RSD (%)	Day 3 Content (μg/mL)	RSD (%)	Inter-day precision ($n = 9$) Content (μg/mL)	RSD (%)
Rubiadin (**1**)[a]	59.75 ± 2.24	3.75	60.52 ± 0.97	1.60	64.67 ± 2.03	3.14	61.64 ± 2.16	3.50
Quercetin (**10**)[b]	56.64 ± 0.6	1.06	56.46 ± 0.7	1.24	56.49 ± 0.9	1.59	56.53 ± 0.08	0.14

[a]Detected in Ben extract.
[b]Detected in EtOAc extract.

Table 4. Recovery data of rubiadin and quercetin from the extracts of *H. pustulata*.

Compound	Added (μg/mL)	Detected[a] (μg/mL)	Mean recovery (%)	RSD (%)
Rubiadin (**1**)	45	44.3 ± 1.2	97.2 ± 2.5	2.57
Quercetin (**10**)	30	29.7 ± 0.4	98.8 ± 1.5	1.52

[a]Calculated by subtracting the total amount after spiking the extracts from the amount in the extracts before spiking. Data were expressed as means of three experiments.

detection (t_R) and quantitation of AQs as well as flavonoids, since all RSD% values in intra- and inter-day precision experiments were less than 4%, and showed a high recovery rate for both kinds of chemical compounds. Therefore, bearing in mind the complex nature of vegetable extracts and the analytical requirements, we can consider this HPLC method suitable for the simultaneous detection and quantitation of AQs and flavonoids in the extracts of *H. pustulata*.

HPLC analysis

The chemical characterization of the extracts by HPLC analysis demonstrated that the Ben extract has only anthraquinone derivatives (Table 5), showing a greater variety of it (Figure 1) at a higher concentration than the other extracts, where the preponderance of rubiadin (**1**) and soranjidiol (**2**) stands out, followed by pustuline (**8**). We also established that the characteristic difference between non-polar and polar extracts is that the latter possess a significant amount of flavonoids.

By analyzing the chemical composition of each extract of *H. pustulata*, the effect produced by it against *C. tropicalis* biofilms can be explained. Thus, the significant antifungal activity of the Ben extract, observed under irradiation (Figure 2), can be attributed to its high content of AQs with photosensitizing properties, since we have established that this effect was due to a high ROS production (Figure 4). It is important to highlight that the rubiadin (**1**) and soranjidiol (**2**) were the predominant AQs in this extract, which have shown to be good photosensitizers by stimulating the $O_2^{\bullet -}$ generation (Type I) (Núñez Montoya et al. 2005; Comini et al. 2007), and this ROS is the main precursor of other oxygen species highly reactive like H_2O_2 and hydroxyl radical ($OH^{\bullet}$). On the other hand, the low-mid concentration of photosensitizing AQs in the Hex, EtOAc and EtOH extracts (Table 5), along with the presence of significant amounts of flavonoids with proven antioxidant properties as quercetin (**10**) and isoquercitrin (**11**) (Permana et al. 2003; Boots et al. 2008) in the polar extracts (EtOAc and EtOH), would be the cause for a low-mid ROS production by these three extracts, and consequently of their inactivity against biofilm.

By applying this validated HPLC method, we established that the AQs with photosensitizing properties (Núñez Montoya et al. 2005; Comini et al. 2007) would be responsible for the effect produced by Ben extract, since only this extract contains exclusively photosensitizing AQs in high concentrations and was the only one that exhibited a significant lowering effect over the biofilm growth by light action. In the case of Hex extract, AQs concentration was lower than in the Ben extract, and would seem that the activation of the total antioxidant system would counteract the effect of the few ROS and RNI generated by the AQs present in this extract. By contrast, EtOAc and EtOH extracts possess a higher content of flavonoids than AQs, two of them with recognized antioxidant activity (quercetin and isoquercitrin) (Permana et al. 2003; Boots et al. 2008). This could explain the low generation of ROS and RNI by these extracts under irradiation, which in turn was counteracted by the activation of the total antioxidant system of the biofilms.

Conclusions

We have demonstrated that the extract obtained from the aerial parts of *H. pustulata*, characterized by a high concentration of AQs exclusively (Ben extract), exhibited a significant reducing effect on the biofilms growth of *C. tropicalis* when it was irradiated. We also established that the slight reduction of the biofilm in darkness was mediated only by a nitrosative stress (increase in the RNI production), whereas under irradiation the oxidative stress was the predominant process (increase in the ROS generation). Therefore, a photodynamic sensitization by this extract was observed, which could be attributed to the high content of photosensitizing AQs, since it has shown that photosensitizers increase the ROS production under irradiation. Thus, a new research line opens up for bioprospecting natural AQs with

Table 5. Identification and quantititation of secondary metabolites in *H. pustulata* extracts by HPLC.

Secondary metabolites Anthraquinones	t_R in extracts (min)	QUANTIFICATION (% P/P)*			
		Hex	Ben	EtOAc	EtOH
Damnacanthol (**6**)	13.85 ± 0.01	–	0.34 ± 0.07	–	–
Soranjidiol 1-methyl ether (**4**)	20.53 ± 0.01	0.014 ± 0.003	0.58 ± 0.08	–	–
Rubiadin 1-methyl ether (**3**)	21.12 ± 0.01	0.05 ± 0.06	0.15 ± 0.08	–	–
2-OH-3-CH_3-AQ (**5**)	23.78 ± 0.04	0.09 ± 0.03	0.30 ± 0.05	0.42 ± 0.12	0.03 ± 0.02
Pustuline (**8**)	23.25 ± 0.05	0.49 ± 0.07	1.64 ± 0.08	0.52 ± 0.01	0.077 ± 0.002
Rubiadin (**1**)	32.57 ± 0.08	0.44 ± 0.14	2.74 ± 0.84	0.416 ± 0.007	0.12 ± 0.02
Soranjidiol (**2**)					
Heterophylline (**7**)	30.9 ± 0.1	0.12 ± 0.09	0.33 ± 0.02	0.038 ± 0.005	–
5,5′-Bisoranjidiol (**9**)	34.4 ± 0.1	0.09 ± 0.05	0.09 ± 0.07	0.06 ± 0.01	–
FLAVONOIDS					
Quercetin (**10**)	11.85 ± 0.04	–	–	2.36 ± 0.03	–
Isoquercitrin (**11**)	8.0 ± 0.2	–	–	1.91 ± 0.07	2.19 ± 0.09
3-*O*-β-D-(6′′-Acetylglucosyl) quercetin (**12**)	9.2 ± 0.1	–	–	3.2 ± 0.4	1.89 ± 0.04

Hex: Hexane extract; Ben: Benzene extract; EtOAc: Ethyl acetate extract; EtOH: Ethanol extract.
*g of compound in 100 g of dried extract.

photosensitizing properties as an alternative to prevent or decrease the formation of biofilms, showing potential use in APDT as antifungal photosensitizers.

Acknowledgements

The authors are thankful to Prof. Dr. G. Barboza (Museo Botánico de Córdoba, Fac. Cs. Exactas y Naturales, and Universidad Nacional de Córdoba) for the identification of the species, and to Dr. M. Bottiglieri for providing the *C. tropicalis* strains.

Disclosure statement

The authors declare no conflict of interest.

Funding information

This work was supported by CONICET, SECyT-UNC, MinCyT and FONCYT. J. Marioni is a research fellow of CONICET. M.G. Paraje, J.L. Cabrera and S.C. Núñez Montoya are members of the Research Career of CONICET-PIP 2013-2015 [GI 4316/2013], SeCyT-UNC [N° 203/14], MinCyT-PID 2008 [N° 121/08 y 35/10] and FONCYT-PICT 2010 [N° 1576].

References

Arce Miranda JE, Sotomayor CE, Albesa I, Paraje MG. 2011. Oxidative and nitrosative stress in *Staphylococcus aureus* biofilm. FEMS Microbiol Lett. 315:23–29.

Bacigalupo NM. 1993. Rubiaceae. In: Cabrera AL, ed. Flora de la Provincia de Jujuy. INTA: Buenos Aires, 375–380.

Baronetti JL, Angel Villegas N, Aiassa V, Paraje MG, Albesa I. 2013. Hemolysin from *Escherichia coli* induces oxidative stress in blood. Toxicon. 70:15–20.

Benzie IFF, Strain JJ. 1996. The ferric reducing ability of plasma (FRAP) as a measure of "antioxidant": the FRAP assay. Anal. Biochem. 239:70–76.

Bizerra FC, Vataru Nakamura C, Poersch C, Estivalet Svidzinski TI, Borsato Quesada RM, Goldenberg S, Krieger MA, Yamada-Ogatta SF. 2008. Characteristics of biofilm formation by *Candida tropicalis* and antifungal resistance. FEMS Yeast Res. 8:442–450.

Boots AW, Haenen GRMM, Bast A. 2008. Health effects of quercetin: from antioxidant to nutraceutical. Eur. J. Pharmacol. 585:325–337.

Clinical and Laboratory Standards Institute (CLSI). 2008. Reference method for broth dilution antifungal susceptibility testing of yeasts; approved standard – third edition. CLSI Document M27-A3 (ISBN 1-56238-666-2). West Wayne (PA): Clinical and Laboratory Standards Institute.

Comini LR, Núñez Montoya SC, Sarmiento M, Cabrera JL, Argüello GA. 2007. Characterizing some photophysical, photochemical and photobiological properties of photosensitizing anthraquinones. J Photochem Photobiol A: Chem. 188:185–191.

Dongxiu H, Bo C, Qingqing T, Shouzhou Y. 2009. Simultaneous determination of five anthraquinones in medicinal plants and pharmaceutical preparations by HPLC with fluorescence detection. J Pharm Biom Anal. 49:1123–1127.

Hansen EW, Martiarena CA. 1967. Contribución al estudio de toxicidad de *Heterophyllaea pustulata* Hook "cegadera" en el ganado. Rev Invest Agrop (INTA). 4:81–113.

Horwitz W. 1982. Evaluation of analytical methods used for regulation of foods and drugs. Anal Chem. 54:67A–76A.

International Conference on Harmonization. 2005a. ICH Q2A: text on validation of analytical procedures. Available at: http://www.fda.gov/downloads/Drugs/GuidanceComplianceRegulatoryInformation/Guidances/ucm073381.pdf. Accessed on August 2015.

International Conference on Harmonization. 2005b. ICH Q2B: talidation of analytical procedures: methodology. Available at: http://www.fda.gov/downloads/Drugs/GuidanceComplianceRegulatoryInformation/Guidances/ucm073384.pdf. Accessed on August 2015

Konigheim BS, Beranek M, Comini LR, Aguilar JJ, Marioni J, Cabrera JL, Contigiani MS, Núñez Montoya SC. 2012. *In vitro* antiviral activity of *Heterophyllaea pustulata* extracts. Nat Prod Commun. 7:1025–1028.

Missall TA, Lodge JK, McEwen JE. 2004. Mechanisms of resistance to oxidative and nitrosative stress: implications for fungal survival in mammalian hosts. Eukaryotic Cell. 3:835–846.

Nithyanand P, Beema Shafreen RM, Muthamil S, Karutha Pandian S. 2015. Usnic acid inhibits biofilm formation and virulent morphological traits of *Candida albicans*. Microbiol Res. 179:20–28.

Núñez Montoya SC, Agnese AM, Cabrera JL. 2006. Anthraquinone derivatives from *Heterophyllaea pustulata*. J Nat Prod. 69:801–803.

Núñez Montoya SC, Agnese AM, Pérez C, Tiraboschi IN, Cabrera JL. 2003. Pharmacological and toxicological activity of *Heterophyllaea pustulata* anthraquinone extracts. Phytomedicine. 10:569–574.

Núñez Montoya SC, Comini LR, Sarmiento M, Becerra C, Albesa I, Argüello GA, Cabrera JL. 2005. Natural anthraquinones probed as Type I and Type II photosensitizers: singlet oxygen and superoxide anion production. J Photochem Photobiol B: Biol. 78:77–83.

Núñez Montoya SC. 2002. Metabolitos secundarios en *Heterophyllaea pustulata* Hook.f. (Rubiáceas). [Ph.D thesis]. National University of Córdoba, Argentina.

O'Toole GA, Kolter R. 1998. Initiation of biofilm formation in *Pseudomonas fluorescens* WCS365 proceeds via multiple, convergent signaling pathways: a genetic analysis. Mol Microbiol. 28:449–461.

Panichayupakaranant P, Sakunpak A, Sakunphueak A. 2009. Quantitative HPLC determination and extraction of anthraquinones in *Senna alata* leaves. J Chromatogr Sci. 47:197–200.

Paraje MG, Correa SG, Albesa I, Sotomayor CE. 2009. Lipase of *Candida albicans* induces activation of NADPH oxidase and l-arginine pathways on resting and activated macrophages. Biochem Biophys Res Commun. 390:263–268.

Peralta MA, da Silva MA, Ortega MG, Cabrera JL, Paraje MG. 2015. Antifungal activity of a prenylated flavonoid from *Dalea elegans* against *Candida albicans* biofilms. Phytomedicine. 22:975–980.

Pereira Gonzaleza F, Maich T. 2012. Photodynamic inactivation for controlling *Candida albicans* infections. Fungal Biol. 116:1–10.

Permana D, Hj Lajisl N, Abas F, Ghafar Othman A, Ahmad R, Kítajima M, Takayama H, Aim N. 2003. Antioxidative constituents of *Hedyotis diffusa* WilLd. Nat Prod Sci. 9:7–9.

Powers SK, Ji A. N, Kavazis LL, Jackson MJ. 2011. Reactive oxygen species: impact on skeletal muscle. Compr Physiol. 1:941–969.

Quattrocchi OA, Abelaira de Anfrizzi SI, Laba RF. 1992. Introducción a la HPLC, Aplicación y Práctica. Buenos Aires, Argentina: Artes Gráficas Farro S.A.

Ramage G, Ranjith R, Leighann S, Craig W. 2012. Fungal biofilm resistance. Int J Microbiol. 2012:528521–528514. Article ID 528521.

Silva S, Negri M, Henriques M, Oliveira R, Williams DW, Azeredo J. 2012. *Candida glabrata*, *Candida parapsilosis* and *Candida tropicalis*: biology, epidemiology, pathogenicity and antifungal resistance. FEMS Microbiol Rev. 36:288–305.

Wei S-Y, Yao W-X, Ji W-Y, Weia J-Q, Peng S-Q. 2013. Qualitative and quantitative analysis of anthraquinones in rhubarbs by high performance liquid chromatography with diode array detector and mass spectrometry. Food Chem. 141:1710–1715.